Science of the Total Environment 923 (2024) 171403

Contents lists available at ScienceDirect

Science of the Total Environment

journal homepage: www.elsevier.com/locate/scitotenv

# Exploring the ecological meanings of temperature sensitivity of ecosystem respiration from different methods

Yang Zhang [a], Gaofeng Zhu [a,*], Kun Zhang [b,*], Heng Huang [c], Liyang He [a], Cong Xu [a], Huiling Chen [d], Yonghong Su [e], Yuzhong Zhang [a], Haochen Fan [a], Boyuan Wang [a]

[a] College of Earth and Environmental Sciences, Lanzhou University, Lanzhou 730000, China
[b] School of Biological Sciences and Institute for Climate and Carbon Neutrality, The University of Hong Kong, Hong Kong SAR, China
[c] School of Ecology, Sun Yat-sen University, Shen Zhen 518107, China
[d] College of Geography and Environmental Sciences, Zhejiang Normal University, Jinhua 321004, China
[e] Northwest Institute of Eco-Environment and Resources, Chinese Academy of Sciences, Lanzhou 730000, China

## HIGHLIGHTS

- Underpinnings and ecological meanings of $Q_{10}$ estimation methods are scrutinized.
- Apparent $Q_{10}$ estimated by long-term method varies across different biomes.
- Short-term and high-frequency signals methods all remove the confounding effect.
- Intrinsic $Q_{10}$ which has removed the confounding effect is convergent.

## GRAPHICAL ABSTRACT

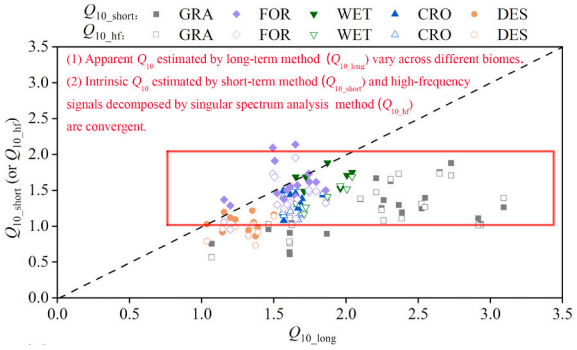


## ARTICLE INFO

Editor: Zhaozhong Feng

*Keywords:*
$Q_{10}$ for $R_e$
Confounding effects
Convergence
Cross-biome

## ABSTRACT

Temperature sensitivity ($Q_{10}$) of ecosystem respiration ($R_e$) is a critical parameter for predicting global terrestrial carbon dynamics and its response to climate warming. However, the determination of $Q_{10}$ has been controversial. In this study, we scrutinized the underpinnings of three mainstream methods to reveal their relationships in estimating $Q_{10}$ for $R_e$ in the Heihe River Basin, northwest China. Specifically, these methods are $Q_{10}$ estimated from the long-term method ($Q_{10\_long}$), short-term method ($Q_{10\_short}$), and the low-frequency ($Q_{10\_lf}$) and high-frequency ($Q_{10\_hf}$) signals decomposed by the singular spectrum analysis (SSA) method. We found that: 1) $Q_{10\_lf}$ and $Q_{10\_long}$ are affected by the confounding effects caused by non-temperature factors, and are 1.8 ± 0.3 and 1.7 ± 0.3, respectively. 2) The high-frequency signals of the SSA method and short-term method have consistent roles in removing the confounding effects. Both $Q_{10\_short}$ and $Q_{10\_hf}$ reflect the actual response of respiration to temperature. 3) Overall, $Q_{10\_long}$ has a larger variability (1.7 ± 0.3) across different biomes, whereas $Q_{10\_short}$ and $Q_{10\_hf}$ show convergence (1.4 ± 0.2 and 1.3 ± 0.1, respectively). These results highlight the fact that $Q_{10}$ can be overestimated by the long-term method, whereas the short-term method and high-frequency signals decomposed by the SSA method can obtain closer and convergent values after removing the confounding

* Corresponding authors at: Lanzhou University, 222 South Tianshui Road, Lanzhou 730000, China.
*E-mail addresses:* zhugf@lzu.edu.cn (G. Zhu), kunzh@hku.hk (K. Zhang).

https://doi.org/10.1016/j.scitotenv.2024.171403
Received 2 January 2024; Received in revised form 23 February 2024; Accepted 28 February 2024
Available online 1 March 2024

effects driven by non-temperature factors. Therefore, it is recommended to use the $Q_{10}$ value estimated by the short-term method or high-frequency signals decomposed by the SSA method to predict carbon dynamics and its response to global warming in Earth system models.

## 1. Introduction

Temperature sensitivity ($Q_{10}$) of ecosystem respiration ($R_e$), which is defined as a quotient of the change in respiration with a 10 °C increase in temperature, is a critical parameter when determining global terrestrial carbon dynamics and its response to climate warming (Karhu et al., 2014; Matteucci et al., 2015; Crowther et al., 2016; Melillo et al., 2017; Niu et al., 2021). Differences in the estimated $Q_{10}$ values can lead to great uncertainties in predicting carbon loss and the intensity of climate-carbon cycle feedback in Earth system models (ESMs) (Johnston et al., 2021; García et al., 2023; Jia et al., 2023). Over the past decades, diverse methods have been proposed to estimate the value of $Q_{10}$ for $R_e$ (Lloyd and Taylor, 1994; Wen et al., 2006; Zhou et al., 2009; Zhang et al., 2022). However, there is still much debate over the estimated $Q_{10}$ values of the different methods (von Lützow and Kögel-Knabner, 2009; Yvon-Durocher et al., 2012; Ding et al., 2016; Wu et al., 2021a). In addition, the relationships between the different methods remain unclear. Therefore, there is a need to compare the different methods, to understand the ecological meanings of $Q_{10}$ estimated by the different methods.

Traditionally, $Q_{10}$ values were directly estimated by fitting the exponential function using observed respiration and temperature data ((Randerson et al., 2009; Graf et al., 2011; Huang and Wang, 2022). Some researchers used year-round observations of respiration and temperature to estimate the $Q_{10}$ value (hereafter named the long-term method), which is an approach that can be affected by other factors (i.e., soil moisture, substrate availability, and vegetation activity) (Bhupinderpal-Singh et al., 2003; Tang et al., 2005; Matteucci et al., 2015; Zhang et al., 2022). Thus, the $Q_{10}$ value estimated by this method is called the "apparent $Q_{10}$" (Davidson et al., 2006). To overcome the shortcomings of this method, Reichstein et al. (2005) proposed to use observations over a successive 15-day period to estimate the $Q_{10}$ value (hereafter named the short-term method), which is considered to represent the actual response of respiration to temperature (Vicca et al., 2009; Curiel Yuste et al., 2010; Wutzler et al., 2018). Overall, the ecological meanings of $Q_{10}$ estimated by short-term and long-term methods are clear and easy to understand. Recently, some researchers have proposed to estimate $Q_{10}$ by the use of a signal decomposition technique, such as singular spectrum analysis (SSA) or empirical mode decomposition (EMD), which decompose the original time series into low-frequency and high-frequency signals (Mahecha et al., 2010; Wang et al., 2010b; Liu et al., 2020; Wu et al., 2023). It is assumed that the confounding effects caused by non-temperature factors exist only in the low-frequency signals, and $Q_{10}$ estimated by the high-frequency signals can represent the actual response of $R_e$ to temperature (Wang et al., 2018; Liu et al., 2020). Thus, the $Q_{10}$ value estimated using the high-frequency signals is called the "intrinsic $Q_{10}$" (Mahecha et al., 2010).

Despite these advances in $Q_{10}$ estimation methods, some obscure problems still exist in the present studies. Firstly, as a signal decomposition method, SSA can decompose the time series into signals with different frequencies (Wang et al., 2018; Liu et al., 2020). As far as the $R_e$ time series is concerned, the ecological meanings of signals with different frequencies decomposed by SSA are not well characterized. Therefore, there is a need to investigate the relationships between the estimated $Q_{10}$ values of the traditional methods and the SSA method. This will help us to understand the ecological meaning of $Q_{10}$ estimated by the SSA method. Secondly, many studies using traditional methods based on year-round observations have shown that the $Q_{10}$ values vary widely at different sites (Wen et al., 2006; Zhou et al., 2009; Yang et al., 2021). The corresponding 95 % confidence ranges of the $Q_{10}$ values range from 2.0 to 2.6 across 60 FLUXNET sites (Mahecha et al., 2010). However, Mahecha et al. (2010) using the high-frequency signals decomposed by the SSA method showed that the value of $Q_{10}$ tends to be convergent (1.4 ± 0.1) across different biomes. Wu et al. (2021a) also diagnosed the convergent $Q_{10}$ across different biomes in north high-latitude regions based on this method. The causes of this divergence of $Q_{10}$ values are not well understood from the standpoint of ecology. Thus, there is an urgent need to compare the $Q_{10}$ values estimated by different methods over diverse biomes, and to verify the convergence of $Q_{10}$ across different biomes.

To solve these issues, we collected data from 15 eddy covariance flux sites with large climate gradients and various landscape types in the Heihe River Basin, northwest China, and estimated their $Q_{10}$ for $R_e$ using the different methods. We assumed that the $Q_{10}$ value estimated from the high-frequency signals decomposed by SSA should be closer to that of the short-term method since both these methods aim to remove the confounding effects driven by non-temperature factors. The specific objectives of this study were: 1) to scrutinize the underpinnings of the three different methods for estimating $Q_{10}$ for $R_e$; 2) to reveal the differences in the $Q_{10}$ values estimated by the different methods; and 3) to explore the convergence *of* $Q_{10}$ across different biomes.

## 2. Materials and methods

### 2.1. Study area

The Heihe River Basin (37°41′N–42°42′N, 96°42′E–102°00′N) is the second-largest inland river basin in China, with a total area of approximately $1.432 \times 10^5$ km$^2$ (Li et al., 2013; Wang et al., 2022) (Fig. 1). The Heihe River originates in the Qilian Mountains and finally disappears in Juyanhai Lake (Li et al., 2018). This basin has distinct cold and arid landscapes from the upper to lower reaches (Liu et al., 2011; Xu et al., 2013; Wang et al., 2019). In the upstream area, typical landscapes for a cold region are found, such as glaciers, alpine grassland, and alpine meadow; the middle reaches are dominated by artificial oasis-riparian zone-wetland-desert compound ecosystems; and the downstream area is dominated by natural oasis and desert (Liu et al., 2018; Wang et al., 2019). Therefore, this basin is an ideal experimental platform for carbon flux research, which also has established integrated observatory networks (Li et al., 2013; Li et al., 2017; Liu et al., 2018).

### 2.2. Data collection and pre-processing

In this basin, 15 sites from the integrated observatory networks were selected for this study, which provided multi-year continuous observations for the eddy covariance fluxes and meteorological elements. The site distribution is shown in Fig. 1 and the detailed information is provided in Table S1. These sites consist of various landscapes, mainly including alpine grassland, alpine meadow, maize, *phragmites australis*, desert steppe, cantaloupe, etc. (Table S1). These sites involve the major ecosystem types for the inland basin, including four grassland sites, three forests sites, one wetland site, two cropland sites, and five desert sites.

A detailed description of the sensors of the eddy covariance system and the automatic weather station for each site can be found in Liu et al. (2018) and Wang et al. (2019). The eddy covariance data pre-processed by EddyPro software and the meteorological data were obtained from the National Tibetan Plateau Data Center (TPDC) (http://data.tpdc.ac.cn/). In addition, soil organic carbon (SOC) content at 0–5 cm at a spatial resolution of 100 m for each site was extracted from the digital

soil mapping dataset of SOC content for the Heihe River Basin, which was also downloaded from the TPDC (Yang et al., 2016). Soil texture data were derived from the World Soil Database (HWSD) (https://www.fao.org/soils-portal/en/), which mainly includes the sand, silt, and clay content (Wang et al., 2009; Yu et al., 2023). The SOC content is rich in the sites of the upstream area, ranging from 48.1 to 58.5 g $kg^{-1}$. In contrast, the sites of middle and downstream areas have less SOC content, and SOC content varies from 1.7 to 9.7 g $kg^{-1}$ (Table S1).

In this study, the gaps in the net $CO_2$ fluxes were filled and the net $CO_2$ fluxes were then partitioned into gross primary productivity (GPP) and ecosystem respiration ($R_e$) by the use of the REddyProc package (Wutzler et al., 2018). The proportion of valid net $CO_2$ fluxes and the number of available years at the 15 sites are provided in Table S2. Only when the proportion of valid values is >70 % can $Q_{10}$ be estimated in that year. As for the Nongtian (NTZ) site, we reduced this proportion limit to 65 % since its observations only cover two years.

### 2.3. Temperature sensitivity ($Q_{10}$) for ecosystem respiration

The temperature sensitivity ($Q_{10}$) for ecosystem respiration is estimated according to the exponential function between ecosystem respiration and air temperature (Mahecha et al., 2010):

$$R_e = R_{ref} Q_{10}^{\frac{T_a - T_{ref}}{\gamma}} \quad (1)$$

where $R_e$ is the mean value of the nighttime ecosystem respiration (μmol $m^{-2}$ $s^{-1}$); $T_a$ is the mean value of the nighttime air temperature (°C); γ is the change in air temperature, which is set to 10 °C; $T_{ref}$ is the reference temperature (15 °C); and $R_{ref}$ is the basic respiration at the reference temperature (μmol $m^{-2}$ $s^{-1}$). The above equation (Eq. (1)) can be linearized by taking the logarithm of two sides as follows:

$$\rho = \rho_{ref} + \tau ln Q_{10} \quad (2)$$

where $\rho = lnR_e$, $\rho_{ref} = lnR_{ref}$, and $\tau = \frac{T_a - T_{ref}}{\gamma}$. The ordinary least squares linear regression method is then used to estimate the values of $Q_{10}$ and $R_{ref}$.

Specifically, in this study, we used year-round observations of respiration and temperature to fit Eq. (2) and obtain the apparent $Q_{10}$ values (hereafter named $Q_{10\_long}$). According to Reichstein et al. (2005), we used a 15-day moving window with a step size of 5 days to divide the whole year's respiration and temperature data into different periods. This window length was short enough to avoid the effects of other factors and long enough to provide adequate data for the regression (Reichstein et al., 2005). Instead of using the original respiration and temperature data in each window, the $Q_{10}$ values were estimated based on the anomalies of respiration and temperature in each 15-day window. The newly generated anomaly series of respiration and temperature in each 15-day window can keep the slope ($lnQ_{10}$) of the linear regression unchanged and help in the comparison with the SSA method. As for each period, the regression parameters and statistics are evaluated after regressions according to the methods described in Reichstein et al. (2005). Only those periods where the relative standard error of the estimates of the parameter $Q_{10}$ is <50 % and where estimates are within an accepted range (0–5) are accepted. These $Q_{10}$ values are thought to constitute the best estimate of the short-term temperature sensitivity of ecosystem respiration, and their mean values are used to estimate the $Q_{10}$ representative for the whole year (hereafter named $Q_{10\_short}$). In this study, the 15-day moving window was also validated in different site-years, due to the similarity of the results, we took a single site (Arou site, ARZ) in 2021 as an example to show the variation of $Q_{10\_short}$ with the increases of window size.

In addition, we used the SSA method to decompose the observed $R_e$ and $T_a$ time series into signals with different frequencies, and estimated the $Q_{10}$ values from the low-frequency (hereafter named $Q_{10\_lf}$) and high-frequency (hereafter named $Q_{10\_hf}$) signals, respectively. The SSA

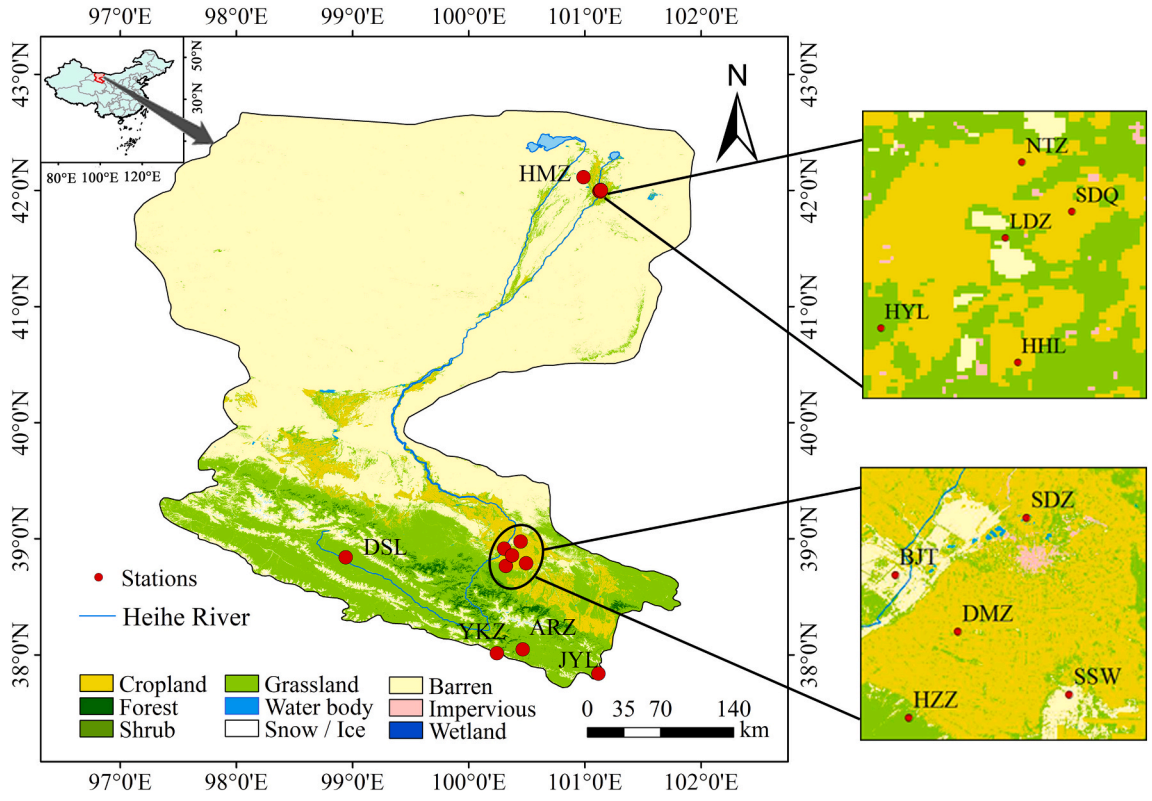


**Fig. 1.** Locations of the 15 eddy covariance flux and meteorological element observation sites in the Heihe River Basin, northwest China. ARZ, DSL, YKZ, JYL, HYL, HHL, SDQ, SDZ, DMZ, NTZ, HZZ, BJT, SSW, HMZ, and LDZ represent the Arou, Dashalong, Yakou, Jingyangling, Huyanglin, Hunhelin, Sidaoqiao, Shidi, Daman, Nongtian, Huazhaizi, Bajitan, Shenshawo, Huangmo, and Luodi sites, respectively.

can decompose the observed time series into the sum of interpretable components with no a priori information about the time series structure (Golyandina and Korobeynikov, 2014). As for a time series $X_N = (x_1, \ldots, x_N)$ of length $N$, let window length $L$ be some integer ($1 < L < N$) and $K=N-L+1$ (Golyandina et al., 2015). The basic processes of the SSA include: 1) mapping the original time series into a sequence of lagged vectors of size $L$ by forming $K=N-L+1$ lagged vectors, and generating the trajectory matrix; 2) determining the eigenvalues and eigenvectors of covariance matrix; 3) calculating the principal components; 4) calculating the reconstructed components of low-frequency and high-frequency signals. In this method, we determine the optimal window length according to the seasonal variation of original time series.

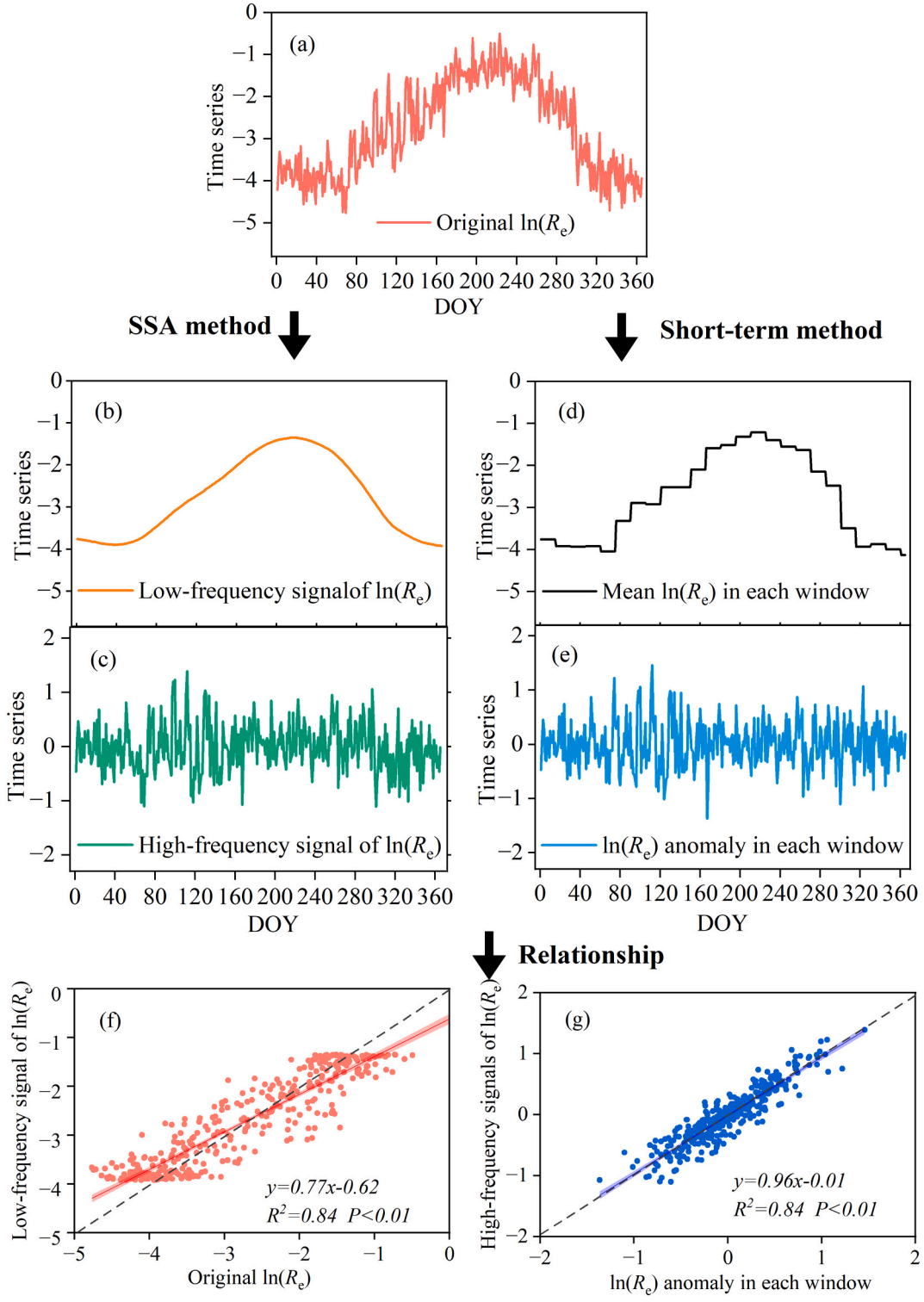


**Fig. 2.** Schematic diagram of the different ln($R_e$) time series and their relationships after being treated with the long-term, short-term, and SSA methods in 2021 in Arou site. (a) show the original ln($R_e$). (b) and (c) show the decomposed low-frequency signal and a high-frequency signal based on the SSA method, respectively. (d) and (e) show the mean ln($R_e$) and ln($R_e$) anomalies in each 15-day window based on the short-term method. (f) show the relationship between the original ln($R_e$) and the low-frequency signal of ln($R_e$). (g) show the relationship between the ln($R_e$) anomaly in each window and the high-frequency band of ln($R_e$).

Specifically, the window length is determined when the reconstructed component of the low-frequency signal from first eigenvalue can best describe the variation trend of time series. Meanwhile, other high-frequency sub-signals are reconstructed as the high-frequency signals. The SSA was performed in MATLAB R2017b (MathWorks Inc., Natick, Ma), and its code can be obtained from the website (https://dept.atmos.ucla.edu/tcd/ssa-tutorial-matlab).

### 2.4. Statistical analysis

The underpinnings of the above three mainstream methods in estimating $Q_{10}$ for $R_e$ (long-term, short-term, and SSA methods) were scrutinized. Annual $R_e$ and $T_a$ time series determined by the three methods performed similar seasonal variation in different site-years. Thus, we took a single site (Arou site, ARZ) as an example to explore their underpinnings. Finally, based on these methods, $Q_{10\_long}$, $Q_{10\_lf}$, $Q_{10\_short}$, and $Q_{10\_hf}$ were estimated for different site-years. As for the magnitude of the confounding effects driven by non-temperature factors, we calculated it as follows:

The confounding effect $= Q_{10\_long} - Q_{10\_short}$ or

The confounding effect $= Q_{10\_long} - Q_{10\_hf}$.

An analysis of variance (ANOVA) of the $Q_{10\_long}$, $Q_{10\_lf}$, $Q_{10\_short}$, and $Q_{10\_hf}$ across different biomes was also conducted using the Duncan multiple range test in SPSS 25.0 (SPSS Inc., Chicago, USA). The correlation analysis between the $Q_{10\_long}$ and $Q_{10\_lf}$, and between $Q_{10\_short}$ and $Q_{10\_hf}$ was conducted in SPSS 25.0 (SPSS Inc., Chicago, USA). All statistical significance level was defined as $P < 0.05$.

## 3. Results

### 3.1. Relationships between the different methods

Taking a single site (Arou site, ARZ) as an example, the different respiration time series ($\rho = lnR_e$) for 2021 and their relationships after being treated with long-term, short-term, and SSA methods are shown in Fig. 2. The original ln($R_e$) in 2021 is decomposed into a low-frequency signal and a high-frequency signal based on the SSA method (Fig. 2a–c). In addition, the mean ln($R_e$) and ln($R_e$) anomalies in each 15-day window based on the short-term method are shown in Fig. 2d–e. Interestingly, it can be found that the low-frequency signal of ln($R_e$) can better reflect the seasonal trend of the original ln($R_e$), which first increased from January to July and then decreased from July to December. In contrast, the high-frequency signal of ln($R_e$) is similar to the ln($R_e$) anomaly in each 15-day window, and both show some oscillation over the short term. The relationship between the original ln($R_e$) and the low-frequency signal of ln($R_e$) can be described by a linear equation (slope = 0.77, $R^2 = 0.84$) (Fig. 2f). Meanwhile, the relationship between the ln($R_e$) anomaly in each window and the high-frequency band of ln($R_e$) can be described by a better linear equation (slope = 0.96, $R^2 = 0.84$) (Fig. 2g). As for the different air temperature time series ($\tau = \frac{T_a - 15}{10}$) for 2021 and their relationships after being treated with the three methods, the characteristics and relationships are similar to the different respiration time series ($\rho = lnR_e$) (Fig. S1).

In addition, we further explored the multi-year variation and relationships of the different respiration/air temperature time series from 2013 to 2021 for the Arou site, and consistent conclusions were obtained, as shown in Figs. S2–S4. Overall, the high-frequency signal of SSA and the time series treated by the short-term method have a consistent role in removing the confounding effects caused by the non-temperature factors. SSA can directly decompose the time series into different frequencies, whereas the short-term method requires a stepwise sliding approach to obtain the $Q_{10}$ value in each window.

### 3.2. The $Q_{10}$ values estimated by the different methods for a single site

The relationships between the $Q_{10}$ values estimated by the different methods over multi-year scales for the Arou site are shown in Fig. 3. Each point refers to the $Q_{10}$ for each year from 2013 to 2021. The results show that $Q_{10\_long}$ is close to $Q_{10\_lf}$ (slope = 1.34, $R^2 = 0.89$), whereas $Q_{10\_short}$ and $Q_{10\_hf}$ are broadly consistent (slope = 0.86, $R^2 = 0.80$). In addition, $Q_{10\_long}$ and $Q_{10\_lf}$ vary over a large range (2.2–3.8), and are affected by the confounding effect driven by non-temperature factors. Whereas $Q_{10\_short}$ and $Q_{10\_hf}$ are relatively convergent and vary over a small range (1.1–1.9) after removing the confounding effect. Notably, $Q_{10\_short}$ and $Q_{10\_hf}$ are still higher in 2020 (1.7 and 1.9, respectively) and 2021 (1.7 and 1.8, respectively). This is affected by significant increasing precipitation in 2020 and 2021 (with precipitation of 743.2–818.7 mm) compared with other years (with precipitation of 392.5–662.1 mm) and thus the original respiration and temperature fluctuated large compared with other years.

### 3.3. The $Q_{10}$ values estimated by the different methods across different biomes

The magnitudes and relationships of the $Q_{10}$ values estimated by the different methods across biomes are shown in Fig. 4 and Table S3. Different points for each biome indicate different site-years. As for the different biomes, it can be found that $Q_{10\_long}$ is close to $Q_{10\_lf}$ and they have a good linear relationship (slope = 1.06, $R^2 = 0.88$). In contrast, $Q_{10\_short}$ and $Q_{10\_hf}$ are broadly consistent and there is also a better linear relationship between them (slope = 0.73, $R^2 = 0.72$).

In addition, the relationship between $Q_{10\_long}$ and $Q_{10\_short}$ (or $Q_{10\_hf}$) in the Heihe River Basin is shown in Fig. 5a. $Q_{10\_long}$ exhibits a considerable degree of variation, with a range spanning from 1.0 to 3.1 and a mean value of 1.7 ± 0.3. Notably, $Q_{10\_long}$ fluctuates more widely in the grassland biome than in the other biomes. In contrast, $Q_{10\_short}$ and $Q_{10\_hf}$ based on the short-term and SSA methods are approximately stable in the range of 0.6–2.1 and 0.6–2.0, respectively. Their mean values are 1.4 ± 0.2 and 1.3 ± 0.1, respectively, and they reflect the actual response of respiration to temperature. As for the magnitude of the confounding effects driven by non-temperature factors, there are large differences across the different biomes (Fig. 5b). Among the different biomes, the grassland ecosystem has the highest confounding effect, with a maximum of 1.0 ± 0.4. Overall, the confounding effect leads to an overestimation of $Q_{10}$ by 0.3 ± 0.3 and 0.5 ± 0.3, respectively, compared with $Q_{10\_short}$ and $Q_{10\_hf}$ in the Heihe River Basin.

## 4. Discussion

### 4.1. The ecological meaning of $Q_{10}$ estimated by the SSA method

Although early studies used high-frequency signals to estimate the response of respiration to temperature, the ecological meanings of $Q_{10}$ estimated by signals with different frequencies remain unclear and difficult to understand (Wang et al., 2010b; Wang et al., 2018). Interestingly, we found that the high-frequency signals of the SSA method and the time series treated by the short-term method have similar variation characteristics (Fig. 2a–e). This results in consistent ecological meanings for $Q_{10\_hf}$ and $Q_{10\_short}$, i.e., both reflect the actual response of respiration to temperature after removing the confounding effects caused by the non-temperature factors (Reichstein et al., 2005; Mahecha et al., 2010). In addition, the low-frequency signal of the SSA method can better reflect the seasonal trend of the original time series, and its estimated $Q_{10}$ value contains the confounding effects caused by the non-temperature factors (Zhou et al., 2009; Mahecha et al., 2010). Therefore, $Q_{10\_lf}$ and $Q_{10\_long}$ are broadly consistent and contain large differences in variation. Overall, this research creatively explains the ecological meanings of $Q_{10}$ estimated by the low-frequency and high-frequency signals.

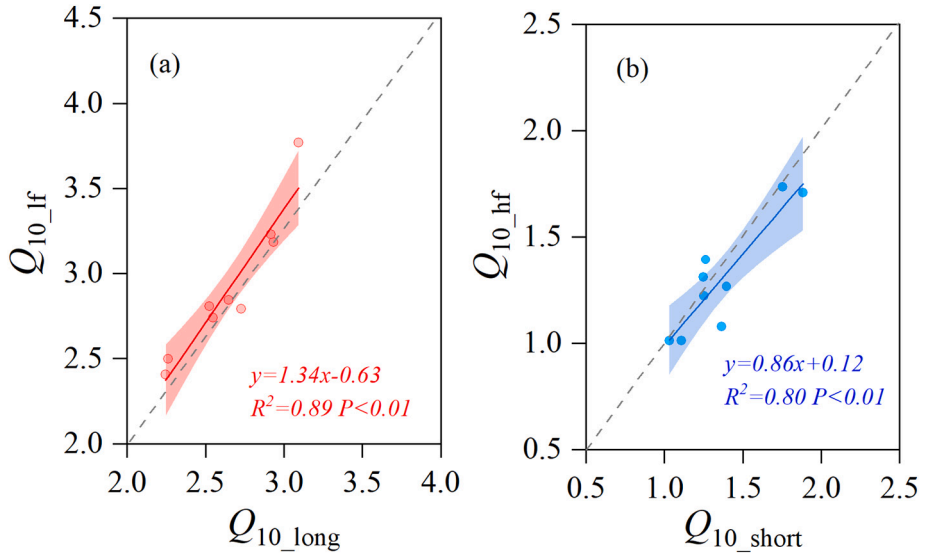


**Fig. 3.** The relationships between (a) the temperature sensitivity estimated by the long-term method ($Q_{10\_long}$) and low-frequency signal ($Q_{10\_lf}$), and (b) the temperature sensitivity estimated by the short-term method ($Q_{10\_short}$) and high-frequency signal ($Q_{10\_hf}$) over multi-year scales. Each point refers to the $Q_{10}$ for each year from 2013 to 2021.

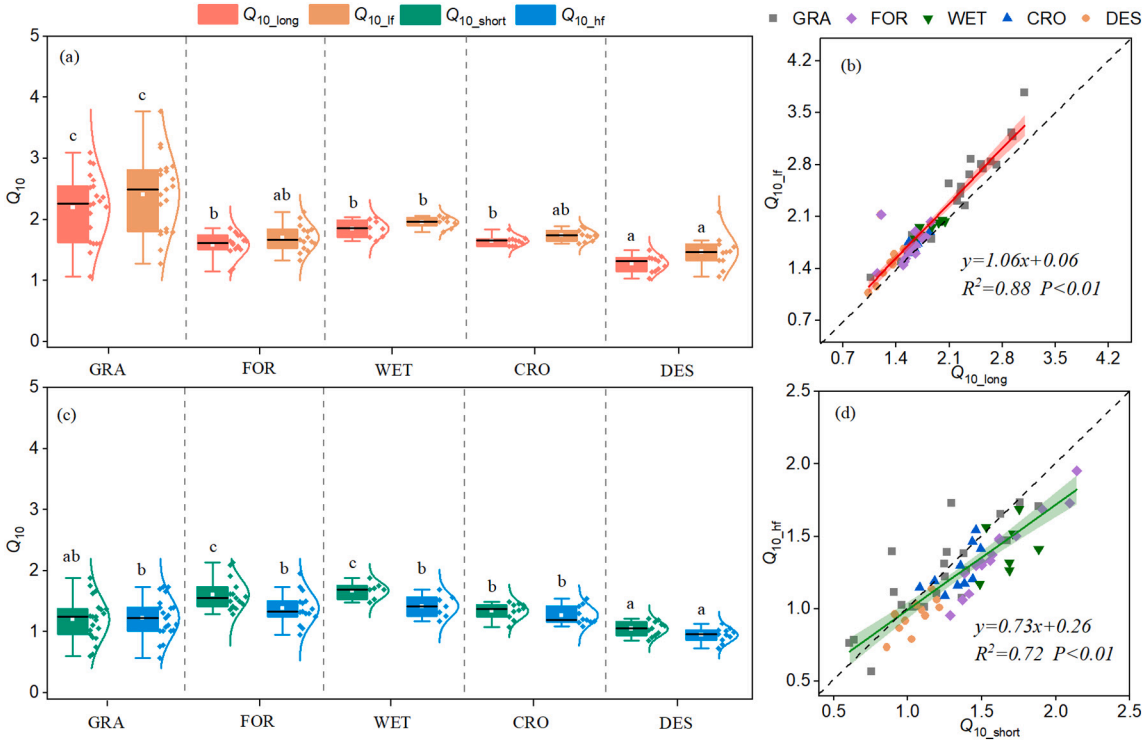


**Fig. 4.** The magnitudes (a and c) and relationships (b and d) of the $Q_{10}$ values estimated by the long-term, short-term, and SSA methods across biomes. The white circles in the boxes indicate the mean values, and the lines across the middle of the boxes indicate the median values. The lower and upper ends of the boxes are the 25th and 75th percentiles. GRA, FOR, WET, CRO, and DES represent the grassland, forest, wetland, cropland, and desert ecosystems, respectively. Different points for each biome indicate different site-years. The different letters above the bars represent the significant difference at $P < 0.05$.

Recently, the convergence of $Q_{10}$ across different biomes has been subject to much debate (Mahecha et al., 2010; Perkins et al., 2012; Gudasz et al., 2021). We found that $Q_{10\_short}$ estimated by the short-term method and $Q_{10\_hf}$ estimated by the high-frequency signal of the SSA method show convergence (1.4 ± 0.2 and 1.3 ± 0.1, respectively) across the different biomes, and are close to the global average values (1.4 ± 0.1) reported by Mahecha et al. (2010). In contrast, $Q_{10\_long}$ estimated by the long-term method shows larger variability (1.7 ± 0.3) across the different biomes. This suggests that the confounding effects caused by the non-temperature factors can result in different estimation values for $Q_{10}$ and can lead to great uncertainty in predicting the temperature response of carbon decomposition (Chen and Tian, 2005; Davidson et al., 2006; Zhou et al., 2009; Wang et al., 2010a).

From a processing perspective, the signal decomposition technique is completely different from the short-term method. The short-term method requires a stepwise sliding approach to estimate $Q_{10}$ in each

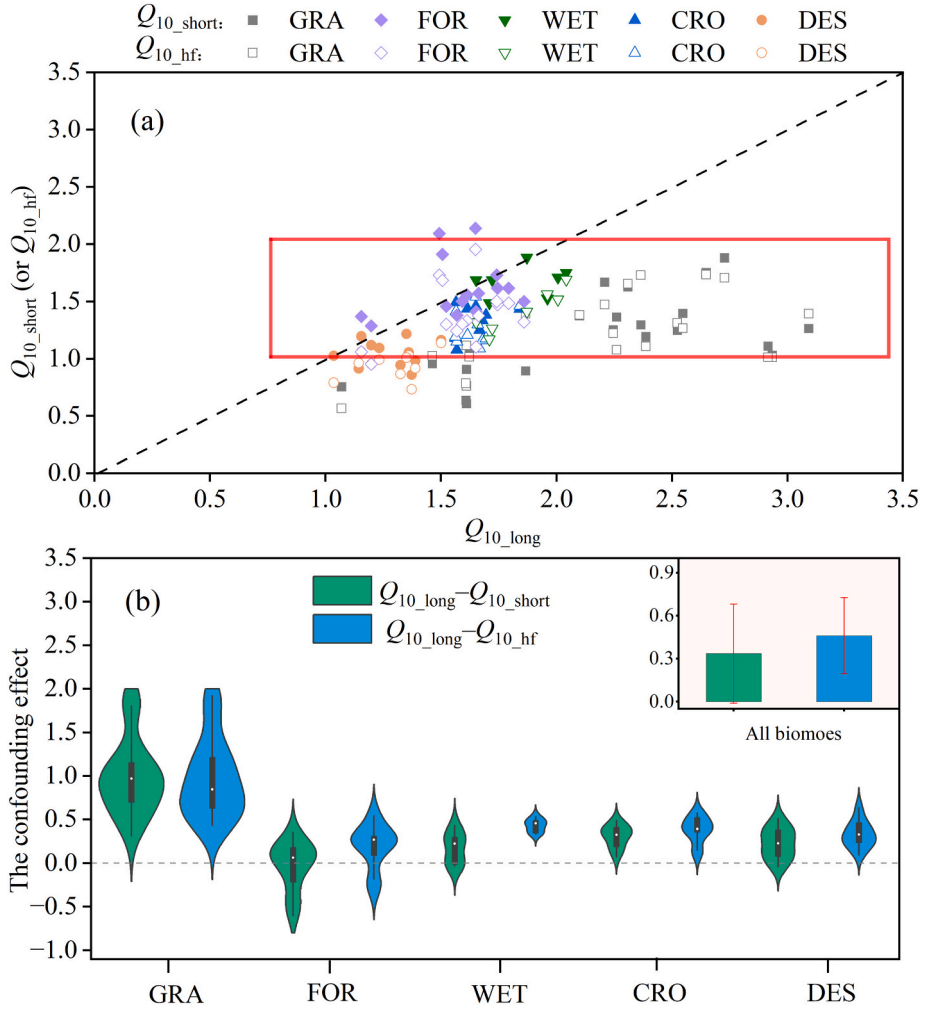


**Fig. 5.** The relationships between the apparent $Q_{10\_long}$ and $Q_{10\_short}$ (or $Q_{10\_hf}$) after removing the confounding effects caused by the non-temperature factors (a) and the confounding effect for $Q_{10}$ (b). GRA, FOR, WET, CRO, and DES represent the grassland, forest, wetland, cropland, and desert ecosystems, respectively. Different points for each biome indicate different site-years.

window, with which it is easy to understand the ecological meaning of $Q_{10}$ (Reichstein et al., 2005). However, this method is susceptible to the outliers within each window, with widely varying $Q_{10}$ estimates from different windows. As for the signal decomposition method, it can quickly decompose the annual time series into high-frequency and low-frequency signals, and directly estimate the actual response of respiration to temperature based on the high-frequency signals. In addition, the long-term method uses year-round data to estimate the apparent $Q_{10}$, which does contain the confounding effect. In the future, the high-frequency signals decomposed by the SSA method could be easily used to estimate the actual response of respiration to temperature.

### 4.2. *Reasons for the wide variation of apparent $Q_{10}$*

To further explore the reasons for the wide variations of apparent $Q_{10}$, we estimated $Q_{10\_short}$ by increasing the window length of the short-term method for the Arou site (Fig. 6). Reichstein et al. (2005) indicated that the 15-day window length is short enough to avoid the effects of other factors and long enough to provide adequate data for the regression. Similarly, we found that the $Q_{10\_short}$ value is stable when the window length is around 10–15. Interestingly, $Q_{10\_short}$ increases and becomes gradually closer to $Q_{10\_long}$ as the window length continues to increase. Therefore, increasing the window length does lead to the entry of other confounding effects caused by the non-temperature factors.

We also explored the relationships between $Q_{10\_long}$ and other factors

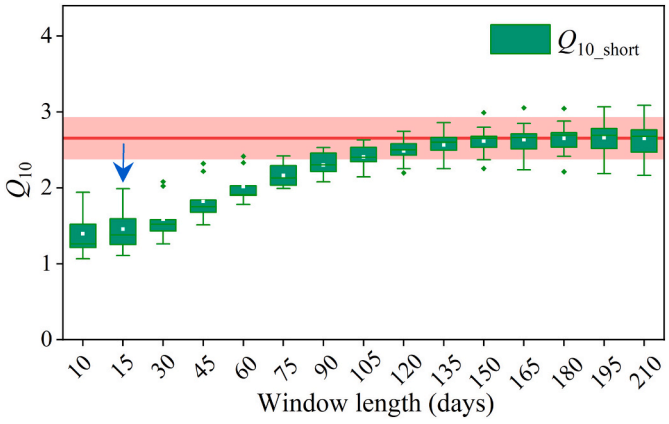


**Fig. 6.** The influence of window length on the temperature sensitivity estimated by the short-term method ($Q_{10\_short}$). The blue arrows represent the 15-day window used in this study. The red line is $Q_{10}$ estimated from the long-term method ($Q_{10\_long}$), and the light-shaded section around the line indicates the standard deviation for the different years.

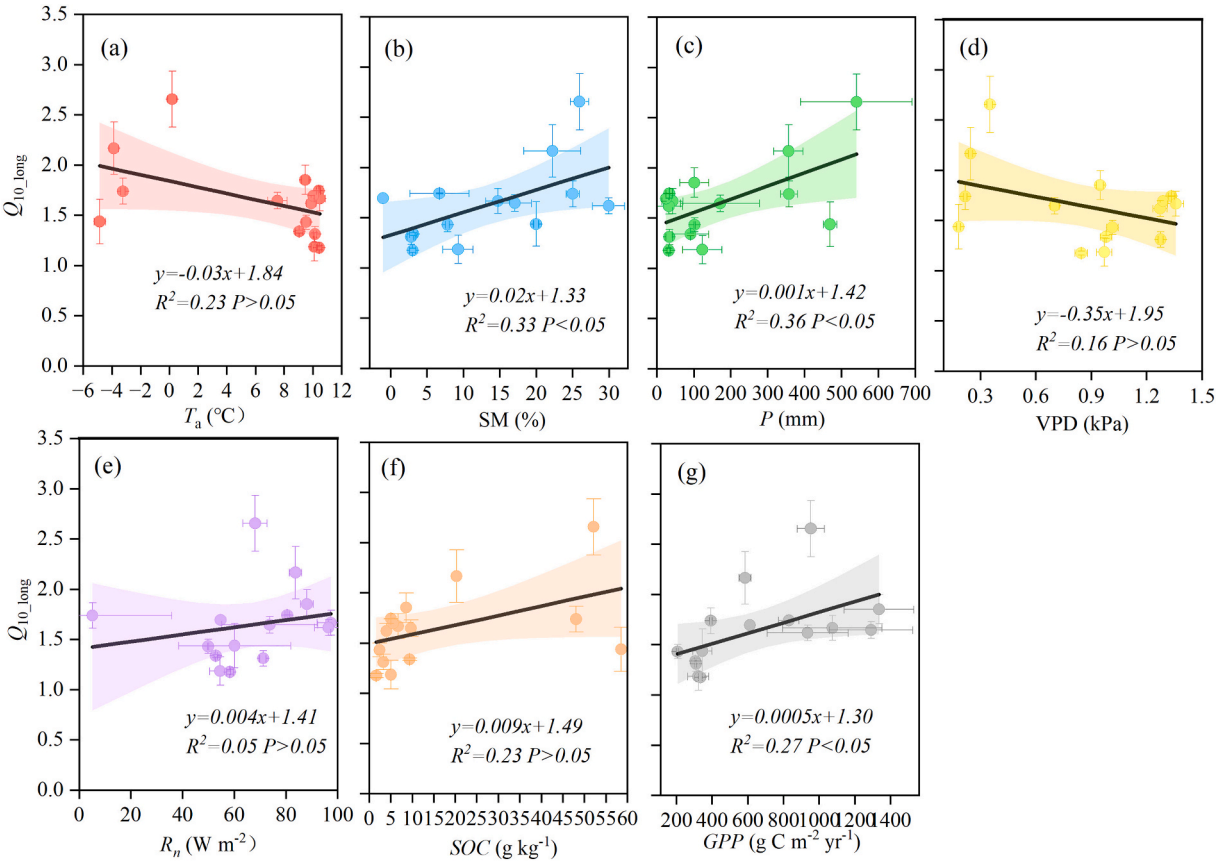


**Fig. 7.** The relationships between $Q_{10\_long}$ and its main influencing factors in the Heihe River Basin. The 15 different points are from the multi-year mean values for each site. The horizontal bars indicate the standard deviation of different years of $Q_{10\_long}$, and the vertical bars indicate the standard deviation of different years of main influencing factors.

(Fig. 7). In this study, we found that precipitation ($P$) and soil moisture (SM) show a strong positive correlation with $Q_{10\_long}$, which suggests that an adequate water supply can promote the temperature response of carbon substrate decomposition (Davidson et al., 2006). In addition, GPP, SOC, and air temperature ($T_a$) are also important factors affecting $Q_{10\_long}$ (Fig. 7). Among these factors, the first two are a prerequisite for an adequate supply of carbon substrates. In the Heihe River Basin, the sites with higher $P$ and SM values are mainly concentrated in the upper reaches, where grassland is common (Fig. S3). There is higher SOC and photosynthetic capacity of vegetation, which provide complex confounding effects to affect the apparent $Q_{10}$ (Figs. S3 and 6b). In addition, our findings confirm the previous results, in that $Q_{10}$ decreases with increasing temperature. The explanation for this negative correlation is that, as temperature increases, there is a declining relative increase in the fraction of organic matter molecules with enough energy to react in chemical reactions (Kirschbaum, 2006; Ågren and Wetterstedt, 2007; Hamdi et al., 2013; Gritsch et al., 2015). Overall, $Q_{10\_long}$ reflects not only the response of $R_e$ to temperature changes, but also the confounding effects of other factors, such as vegetation growth (e.g., roots and leaves), substrate supply, and other environmental changes (e.g., SM) (Gaumont-Guay et al., 2009; Gritsch et al., 2015; Chang et al., 2016; Yan et al., 2019).

### 4.3. The $Q_{10}$ values in Earth system models

Differences in the estimated $Q_{10}$ values can lead to great uncertainties in predicting the intensity of climate-carbon cycle feedback in ESMs. Previous studies usually obscured the $Q_{10}$ obtained from different methods, especially long-term method even didn't account for the confounding effect (Mahecha et al., 2010; Wu et al., 2021a). In addition, the temperature increase experiment is also used to explore the independent response of carbon dynamics to global warming (Chen et al., 2022; Wang et al., 2021). However, it is still difficult to fully conform to the real situation in the field since there are many influencing factors with covariation effects (Zhang et al., 2022). In this study, the $Q_{10}$ values estimated by the short-term method and high-frequency signals decomposed by the SSA method provide us with the possibility of exploring a true response of $R_e$ to $T_a$ under long-term observations rather than control experiments (Reichstein et al., 2005; Wu et al., 2021a). The high-frequency signals of the SSA method and short-term method have consistent roles in removing the confounding effect, and they are applicable to all biomes. Thus, we can quickly obtain reliable $Q_{10}$ values based on the high-frequency signals of the SSA method and short-term method.

Although some studies have given the $Q_{10}$ values obtained using different methods, the $Q_{10}$ values are not distinguished explicitly in ESMs (Smith and Dukes, 2013; Shao et al., 2013; Foereid et al., 2014; Badawy et al., 2016; Todd-Brown et al., 2018; Wu et al., 2021b). Previous studies have shown that the $Q_{10}$ values in the ESMs in the Coupled Model Intercomparison Project 5 (CMIP5) range from 1.4 to 2.2 (Todd-Brown et al., 2018; Hashimoto et al., 2015). We further investigated the differences of $Q_{10}$ in some specific models (Table 1). Most models typically set $Q_{10}$ as a constant value of 2, e.g., the Terrestrial Ecosystem Model (TEM) and the Carnegie-Ames-Stanford Approach (CASA) model (Tjoelker et al., 2001; Liu et al., 2016). Only very few models employ a fixed value of 1.5 as $Q_{10}$ (e.g., in the Community Land Model, CLM) (Oleson et al., 2013; Foereid et al., 2014; Meyer et al., 2018), which is close to the global results (1.4 ± 0.1) reported by Mahecha et al. (2010), and also our results. As a result, the response of carbon emissions to climate warming can be overestimated, and there is therefore an urgent

**Table 1**
Detailed $Q_{10}$ values for the carbon decomposition settings in different models.

| Model | $Q_{10}$ | References |
|---|---|---|
| Carnegie-Ames-Stanford Approach (CASA) Biosphere model | 2 | Potter et al. (1993) |
| Community Land Model (CLM) | 1.5 | Foereid et al. (2014); Wieder et al. (2014) |
| Terrestrial Ecosystem Model (TEM) | 2 | Raich et al. (1991); Tian et al. (1999); Chen and Zhuang (2013) |
| Photosynthetic/ Evapotranspiration model (PnET) | 2 | Aber and Federer (1992); Thorn et al. (2015) |
| MONTHLYC model | 2 | Box (1988); Alexandrov (2014) |
| Simple canopy-scale carbon balance model | 2 | Thomas et al. (2019) |
| Boreal Ecosystem Productivity Simulator (BEPS) | 2 | Chen et al. (1999); Chen et al. (2017) |
| ORCALIM ocean and sea ice model | 2 | Friedlingstein et al. (2006) |
| Max Planck Institute for Meteorology (MPI) model | 1.5 | Friedlingstein et al. (2006) |
| The University of Maryland (UMD) Coupled Atmosphere-Biosphere-Ocean (CABO) model | 2.2 for the fast pool, 1.35 for the intermediate pool, and 1.1 for the slow pool | Friedlingstein et al. (2006) |
| TRIFFID dynamic vegetation model | 2 | Friedlingstein et al. (2006) |
| Marine Biogeochemistry Library (MARBL) of the Community Earth System Model, version 2 (CESM2) | 1.7 | Long et al. (2021) |
| HadGEM2-CC | 1.9 | Coleman and Jenkinson (2014); Todd-Brown et al. (2018) |
| HadGEM2-ES | 1.8 | Collins et al. (2011); Todd-Brown et al. (2018) |
| INM-CM4 | 2 | Bonan (1996) |
| IPSL-CM5A-MR | 2 | Volodin (2007); Todd-Brown et al. (2018) |

need to adjust the appropriate setting of $Q_{10}$ in most ESMs (Wang et al., 2010b).

## 5. Conclusions

In this study, we scrutinized the underpinnings of three mainstream methods (long-term, short-term, and SSA methods) to reveal their relationships in estimating $Q_{10}$ for $R_e$ in the Heihe River Basin, northwest China. We found that the high-frequency signal of the SSA method and the time series treated by the short-term method show similar variation characteristics. This results in consistent ecological meanings for $Q_{10\_hf}$ and $Q_{10\_short}$. $Q_{10\_hf}$ and $Q_{10\_short}$ show convergence ($1.4 \pm 0.2$ and $1.3 \pm 0.1$, respectively) and reflect the actual response of respiration to temperature after removing the confounding effects caused by the non-temperature factors. In addition, the low-frequency signal of the SSA method can better reflect the seasonal variation of the original time series, and its estimated $Q_{10}$ value contains the confounding effects caused by the non-temperature factors. Therefore, the $Q_{10}$ values estimated by the low-frequency signal of the SSA or long-term method show large differences across different biomes ($1.7 \pm 0.3$). Overall, the short-term and SSA methods can obtain closer and convergent values after removing the confounding effects. Therefore, it is recommended to use $Q_{10}$ obtained by the latter two methods to predict the terrestrial carbon dynamics and its response to global warming in ESMs.

## CRediT authorship contribution statement

**Yang Zhang:** Conceptualization, Writing–Original draft. **Gaofeng Zhu:** Writing–Reviewing and Editing, Funding acquisition. **Kun Zhang:** Writing–Reviewing and Editing. **Heng Huang:** Writing–Reviewing and Editing. **Liyang He:** Formal analysis. **Cong Xu:** Methodology. **Huiling Chen:** Formal analysis. **Yonghong Su:** Visualization, Funding acquisition. **Yuzhong Zhang:** Formal analysis. **Haochen Fan:** Formal analysis. **Boyuan Wang:** Formal analysis.

## Declaration of competing interest

The authors declare that they have no competing financial interests or personal relationships that could have appeared to influence the work reported in this paper.

## Data availability

Data will be made available on request.

## Acknowledgements

This research was funded by the Key Project of Natural Science Foundation of Gansu province (grant no. 23JRRA1025) and the National Natural Science Foundation of China (grant nos. 42171019 and 42071138). The field measurement data were provided by the National Tibetan Plateau Data Center (http://data.tpdc.ac.cn), which we would very much like to thank.

## Appendix A. Supplementary data

Supplementary data to this article can be found online at https://doi.org/10.1016/j.scitotenv.2024.171403.

## References

Aber, J.D., Federer, C.A., 1992. A generalized, lumped-parameter model of photosynthesis, evapotranspiration and net primary production in temperate and boreal forest ecosystems. Oecologia 92 (4), 463–474. https://doi.org/10.1007/BF00317837.

Ågren, G.I., Wetterstedt, J.Å.M., 2007. What determines the temperature response of soil organic matter decomposition? Soil Biol. Biochem. https://doi.org/10.1016/j.soilbio.2007.02.007.

Alexandrov, G.A., 2014. Explaining the seasonal cycle of the globally averaged CO2 with a carbon-cycle model. Earth Syst. Dynam. 5 (2), 345–354. https://doi.org/10.5194/esd-5-345-2014.

Badawy, B., Arora, V.K., Melton, J.R., Nassar, R., 2016. Journal of advances in modeling earth systems. Journal of Advances in Modeling Earth Systems. 8, 614–633. https://doi.org/10.1002/2015MS000540.

Bhupinderpal-Singh, Nordgren, A., Löfvenius, M.O., Högberg, M.N., Mellander, P.E., Högberg, P., 2003. Tree root and soil heterotrophic respiration as revealed by girdling of boreal scots pine forest: extending observations beyond the first year. Plant, Cell Environ. 26 (8), 1287–1296. https://doi.org/10.1046/j.1365-3040.2003.01053.x.

Bonan, G.B., 1996. Ecological, Hydrological, and Atmospheric Studies: Technical Description and User's Guide (Ncar/Tn-417+Str Ncar Technical Note, 150 pp.).

Box, E.O., 1988. Estimating the seasonal carbon source-sink geography of a natural, steady-state terrestrial biosphere. J. Appl. Meteorol. https://doi.org/10.1175/1520-0450(1988)027<1109:etscss>2.0.co;2.

Chang, S.X., Shi, Z., Thomas, B.R., 2016. Soil respiration and its temperature sensitivity in agricultural and afforested poplar plantation systems in northern Alberta. Biol. Fertil. Soils 52 (5), 629–641. https://doi.org/10.1007/s00374-016-1104-x.

Chen, H., Tian, H.Q., 2005. Does a general temperature-dependent Q10 model of soil respiration exist at biome and global scale? J. Integr. Plant Biol. 47 (11), 1288–1302. https://doi.org/10.1111/j.1744-7909.2005.00211.x.

Chen, J.M., Liu, J., Cihlar, J., Goulden, M.L., 1999. Daily canopy photosynthesis model through temporal and spatial scaling for remote sensing applications. Ecol. Model. 124 (2–3), 99–119. https://doi.org/10.1016/s0304-3800(99)00156-8.

Chen, M., Zhuang, Q., 2013. Modelling temperature acclimation effects on the carbon dynamics of forest ecosystems in the conterminous United States. Tellus B Chem. Phys. Meteorol. 65 (1) https://doi.org/10.3402/tellusb.v65i0.19156.

Chen, Z., Chen, J.M., Zhang, S., Zheng, X., Ju, W., Mo, G., Lu, X., 2017. Optimization of terrestrial ecosystem model parameters using atmospheric CO2 concentration data with the global carbon assimilation system (GCAS). J. Geophys. Res. Biogeo. 122 (12), 3218–3237. https://doi.org/10.1002/2016JG003716.

Coleman, K., Jenkinson, D., 2014. RothC - A model for the turnover of carbon in soil (windows version) (updated June 2014), (June), 44. https://www.rothamsted.ac.uk/sites/default/files/RothC_guide_WIN.pdf.
Collins, W.J., Bellouin, N., Doutriaux-Boucher, M., Gedney, N., Halloran, P., Hinton, T., et al., 2011. Development and evaluation of an earth-system model - HadGEM2. Geosci. Model Dev. 4 (4), 1051–1075. https://doi.org/10.5194/gmd-4-1051-2011.
Crowther, T.W., Todd-Brown, K.E.O., Rowe, C.W., Wieder, W.R., Carey, J.C., MacHmuller, M.B., et al., 2016. Quantifying global soil carbon losses in response to warming. Nature 540 (7631), 104–108. https://doi.org/10.1038/nature20150.
Curiel Yuste, J., Ma, S., Baldocchi, D.D., 2010. Plant-soil interactions and acclimation to temperature of microbial-mediated soil respiration may affect predictions of soil CO2 efflux. Biogeochemistry 98 (1–3), 127–138. https://doi.org/10.1007/s10533-009-9381-1.
Davidson, E.A., Janssens, I.A., Lou, Y., 2006. On the variability of respiration in terrestrial ecosystems: moving beyond Q10. Glob. Chang. Biol. 12 (2), 154–164. https://doi.org/10.1111/j.1365-2486.2005.01065.x.
Ding, J., Chen, L., Zhang, B., Liu, L., Yang, G., Fang, K., et al., 2016. Global biogeochemical cycles. Global Biogeochem. Cycles 30, 1310–1323. https://doi.org/10.1002/2015GB005333.Received.
Foereid, B., Ward, D.S., Mahowald, N., Paterson, E., Lehmann, J., 2014. The sensitivity of carbon turnover in the community land model to modified assumptions about soil processes. Earth Syst. Dynam. 5 (1), 211–221. https://doi.org/10.5194/esd-5-211-2014.
Friedlingstein, P., Betts, R., Bopp, L., Bloh, W. Von, Brovkin, V., Doney, S., et al., 2006. Climate –carbon cycle feedback analysis, results from the C4MIP model intercomparison. J. Climate 19, 3337–3353. https://doi.org/10.1175/JCLI3800.1.
García, F.C., Clegg, T., O'Neill, D.B., Warfield, R., Pawar, S., Yvon-Durocher, G., 2023. The temperature dependence of microbial community respiration is amplified by changes in species interactions. Nat. Microbiol. 8 (2), 272–283. https://doi.org/10.1038/s41564-022-01283-w.
Gaumont-Guay, D., Black, T.A., McCaughey, H., Barr, A.G., Krishnan, P., Jassal, R.S., Nesic, Z., 2009. Soil CO2 efflux in contrasting boreal deciduous and coniferous stands and its contribution to the ecosystem carbon balance. Glob. Chang. Biol. 15 (5), 1302–1319. https://doi.org/10.1111/j.1365-2486.2008.01830.x.
Golyandina, N., Korobeynikov, A., 2014. Basic singular Spectrum analysis and forecasting with R. Computational Statistics and Data Analysis 71, 934–954. https://doi.org/10.1016/j.csda.2013.04.009.
Golyandina, N., Korobeynikov, A., Shlemov, A., Usevich, K., 2015. Multivariate and 2D extensions of singular spectrum analysis with the Rssa package. J. Stat. Softw. 67 (2) https://doi.org/10.18637/jss.v067.i02.
Chen, Y., Han, M., Yuan, X., Hou, Y., Qin, W., Zhou, H., Zhao, X., Klein, J.A., Zhu, B., 2022. Warming has a minor effect on surface soil organic carbon in alpine meadow ecosystems on the Qinghai–Tibetan Plateau. Glob. Chang. Biol. 28, 1618–1629. https://doi.org/10.1111/gcb.15984.
Graf, A., Weihermüller, L., Huisman, J. A., Herbst, M., & Vereecken, H. (2011). Comment on "Global convergence in the temperature sensitivity of respiration at ecosystem level." Science, 331(6022). https://doi.org/10.1126/science.1196948.
Gritsch, C., Zimmermann, M., Zechmeister-Boltenstern, S., 2015. Interdependencies between temperature and moisture sensitivities of CO2 emissions in European land ecosystems. Biogeosciences 12 (20), 5981–5993. https://doi.org/10.5194/bg-12-5981-2015.
Gudasz, C., Karlsson, J., Bastviken, D., 2021. When does temperature matter for ecosystem respiration? Environmental research. Communications 3 (12). https://doi.org/10.1088/2515-7620/ac3b9f.
Hamdi, S., Moyano, F., Sall, S., Bernoux, M., Chevallier, T., 2013. Synthesis analysis of the temperature sensitivity of soil respiration from laboratory studies in relation to incubation methods and soil conditions. Soil Biol. Biochem. 58, 115–126. https://doi.org/10.1016/j.soilbio.2012.11.012.
Hashimoto, S., Carvalhais, N., Ito, A., Migliavacca, M., Nishina, K., Reichstein, M., 2015. Global spatiotemporal distribution of soil respiration modeled using a global database. Biogeosciences 12 (13), 4121–4132. https://doi.org/10.5194/bg-12-4121-2015.
Huang, Y., Wang, Y., 2022. Carbon turnover gets wet. Nat. Geosci. 15 (12), 960–961. https://doi.org/10.1038/s41561-022-01098-8.
Jia, J., Liu, Z., Haghipour, N., Wacker, L., Zhang, H., Sierra, C. A., et al. (2023). Molecular 14 C evidence for contrasting turnover and temperature sensitivity of soil organic matter components . Ecology Letters, (December 2022), 778–788. https://doi.org/10.1111/ele.14204.
Johnston, A.S.A., Meade, A., Ardö, J., Arriga, N., Black, A., Blanken, P.D., et al., 2021. Temperature thresholds of ecosystem respiration at a global scale. Nature Ecology and Evolution 5 (4), 487–494. https://doi.org/10.1038/s41559-021-01398-z.
Karhu, K., Auffret, M.D., Dungait, J.A.J., Hopkins, D.W., Prosser, J.I., Singh, B.K., et al., 2014. Temperature sensitivity of soil respiration rates enhanced by microbial community response. Nature 513 (7516), 81–84. https://doi.org/10.1038/nature13604.
Kirschbaum, M.U.F., 2006. The temperature dependence of organic-matter decomposition - still a topic of debate. Soil Biol. Biochem. 38 (9), 2510–2518. https://doi.org/10.1016/j.soilbio.2006.01.030.
Li, X., Cheng, G., Liu, S., Xiao, Q., Ma, M., Jin, R., et al., 2013. Heihe watershed allied telemetry experimental research (HiWater) scientific objectives and experimental design. Bull. Am. Meteorol. Soc. 94 (8), 1145–1160. https://doi.org/10.1175/BAMS-D-12-00154.1.
Li, X., Cheng, G., Ge, Y., Li, H., Han, F., Hu, X., et al., 2018. Hydrological cycle in the Heihe River basin and its implication for water resource Management in Endorheic Basins. J. Geophys. Res. Atmos. 123 (2), 890–914. https://doi.org/10.1002/2017JD027889.
Li, X., Liu, S., Xiao, Q., Ma, M., Jin, R., Che, T., Wang, W., Hu, X., Xu, Z., Wen, J., Wang, L., 2017. A multiscale dataset for understanding complex eco-hydrological processes in a heterogeneous oasis system. Sci. Data 4, 1–11. https://doi.org/10.1038/sdata.2017.83.
Liu, P., Zha, T., Jia, X., Bourque, C, P.-A., Tian, Y., Ma, J., et al., 2020. Soil respiration sensitivity to temperature in biocrusted soils in a desert-shrubland ecosystem. Catena 191 (December 2019), 104556. https://doi.org/10.1016/j.catena.2020.104556.
Liu, S., Xu, Z., Wang, W., Jia, Z., Zhu, M., Bai, J., Wang, J., 2011. A comparison of eddy-covariance and large aperture scintillometer measurements with respect to the energy balance closure problem. Hydrol. Earth Syst. Sci. 15 (4), 1291–1306. https://doi.org/10.5194/hess-15-1291-2011.
Liu, S., Li, X., Xu, Z., Che, T., Xiao, Q., Ma, M., et al., 2018. The Heihe integrated observatory network: A basin-scale land surface processes Observatory in China. Vadose Zone J. 17 (1), 1–21. https://doi.org/10.2136/vzj2018.04.0072.
Liu, Y., Wang, T., Huang, M., Yao, Y., Ciais, P., Piao, S., 2016. Changes in interannual climate sensitivities of terrestrial carbon fluxes during the 21st century predicted by CMIP5 earth system models. J. Geophys. Res. Biogeo. 121 (3), 903–918. https://doi.org/10.1002/2015JG003124.
Lloyd, J., Taylor, J.A., 1994. On the temperature dependence of soil respiration. Funct. Ecol. 8 (3), 315. https://doi.org/10.2307/2389824.
Long, M.C., Moore, J.K., Lindsay, K., Levy, M., Doney, S.C., Luo, J.Y., et al., 2021. Simulations with the marine biogeochemistry library (MARBL). Journal of Advances in Modeling Earth Systems 13 (12). https://doi.org/10.1029/2021MS002647.
Mahecha, M.D., Reichstein, M., Carvalhais, N., Lasslop, G., Lange, H., Seneviratne, S.I., et al., 2010. Global convergence in the temperature sensitivity of respiration at ecosystem level. Science 329 (5993), 838–840. https://doi.org/10.1126/science.1189587.
Matteucci, M., Gruening, C., Goded Ballarin, I., Seufert, G., Cescatti, A., 2015. Components, drivers and temporal dynamics of ecosystem respiration in a Mediterranean pine forest. Soil Biol. Biochem. 88, 224–235. https://doi.org/10.1016/j.soilbio.2015.05.017.
Melillo, J.M., Frey, S.D., DeAngelis, K.M., Werner, W.J., Bernard, M.J., Bowles, F.P., et al., 2017. Long-term pattern and magnitude of soil carbon feedback to the climate system in a warming world. Science 358 (6359), 101–105. https://doi.org/10.1126/science.aan2874.
Meyer, N., Welp, G., Amelung, W., 2018. The temperature sensitivity (Q10) of soil respiration: controlling factors and spatial prediction at regional scale based on environmental soil classes. Global Biogeochem. Cycles 32 (2), 306–323. https://doi.org/10.1002/2017GB005644.
Niu, B., Zhang, X., Piao, S., Janssens, I.A., Fu, G., He, Y., et al., 2021. Warming homogenizes apparent temperature sensitivity of ecosystem respiration. Science. Advances 7 (15), eabc7358. https://doi.org/10.1126/sciadv.abc7358.
Oleson, K.W., Lawrence, D.M., Bonan, G.B., Drewniak, B., Huang, M., Koven, C.D., Levis, S., Li, F., Riley, W.J., Subin, Z.M., Swenson, S.C., Thornton, P.E., Bozbiyik, A., Fisher, R., Heald, C.L., Kluzek, E., Lamarque, J.F., Lawrence, P.J., Leung, R., Lipscomb, W., Muszala, S., Ricciuto, D.M., Sacks, W., Sun, Y., Tang, J., Yang, Z.L., 2013. Technical Description of the Version 4.5 of the Community Land Model (CLM), No. NCAR/TN-503+STR. https://doi.org/10.5065/D6RR1W7M.
Perkins, D.M., Yvon-Durocher, G., Demars, B.O.L., Reiss, J., Pichler, D.E., Friberg, N., et al., 2012. Consistent temperature dependence of respiration across ecosystems contrasting in thermal history. Glob. Chang. Biol. 18 (4), 1300–1311. https://doi.org/10.1111/j.1365-2486.2011.02597.x.
Potter, S., Randerson, T., Field, B., Matson, A., Mooney, H.A., 1993. Terrestrial ecosystem production: a process model based on global satellite and surface data 7 (4), 811–841.
Raich, A. J. W., Rastetter, E. B., Melillo, J. M., Kicklighter, D. W., Steudler, P. A., Grace, A. L., et al. (1991). Potential Net Primary Productivity in South America: Application of a Global Model Published by: Ecological Society of America Stable URL: http://www.jstor.org/stable/1941899 . POTENTIAL NET PRIMARY PRODUCTIVITY IN SOUTH AMERICA: APPLICATION OF A GLOB. Ecol. Appl., 1(4), 399–429. Retrieved from http://www.jstor.org/stable/1941899.
Randerson, J.T., Hoffman, F.M., Thornton, P.E., Mahowald, N.M., Lindsay, K., Lee, Y.H., et al., 2009. Systematic assessment of terrestrial biogeochemistry in coupled climate-carbon models. Glob. Chang. Biol. 15 (10), 2462–2484. https://doi.org/10.1111/j.1365-2486.2009.01912.x.
Reichstein, M., Falge, E., Baldocchi, D., Papale, D., Aubinet, M., Berbigier, P., et al., 2005. On the separation of net ecosystem exchange into assimilation and ecosystem respiration: review and improved algorithm. Glob. Chang. Biol. 11 (9), 1424–1439. https://doi.org/10.1111/j.1365-2486.2005.001002.x.
Shao, P., Zeng, X., Moore, D.J.P., Zeng, X., 2013. Soil microbial respiration from observations and earth system models. Environ. Res. Lett. 8 (3) https://doi.org/10.1088/1748-9326/8/3/034034.
Smith, N.G., Dukes, J.S., 2013. Plant respiration and photosynthesis in global-scale models: incorporating acclimation to temperature and CO2. Glob. Chang. Biol. 19 (1), 45–63. https://doi.org/10.1111/j.1365-2486.2012.02797.x.
Tang, J., Baldocchi, D.D., Xu, L., 2005. Tree photosynthesis modulates soil respiration on a diurnal time scale. Glob. Chang. Biol. 11 (8), 1298–1304. https://doi.org/10.1111/j.1365-2486.2005.00978.x.
Thomas, R.Q., Williams, M., Cavaleri, M.A., Exbrayat, J.F., Smallman, T.L., Street, L.E., 2019. Alternate trait-based leaf respiration schemes evaluated at ecosystem-scale through carbon optimization modeling and canopy property data. Journal of Advances in Modeling Earth Systems 11 (12), 4629–4644. https://doi.org/10.1029/2019MS001679.

Thorn, A.M., Xiao, J., Ollinger, S.V., 2015. Generalization and evaluation of the process-based forest ecosystem model PnET-CN for other biomes. Ecosphere 6 (3), 1–27. https://doi.org/10.1890/ES14-00542.1.

Tian, H., Melillo, J.M., Kicklighter, D.W., Mcguire, A.D., Helfrich, J., 1999. The sensitivity of terrestrial carbon storage to historical climate variability and atmospheric CO2 in the United States. Tellus B Chem. Phys. Meteorol. 51 (2), 414–452. https://doi.org/10.3402/tellusb.v51i2.16318.

Tjoelker, M.G., Oleksyn, J., Reich, P.B., 2001. Modelling respiration of vegetation: evidence for a general temperature-dependent Q10. Glob. Chang. Biol. 7 (2), 223–230. https://doi.org/10.1046/j.1365-2486.2001.00397.x.

Todd-Brown, K., Zheng, B., Crowther, T.W., 2018. Field-warmed soil carbon changes imply high 21st-century modeling uncertainty. Biogeosciences 15 (12), 3659–3671. https://doi.org/10.5194/bg-15-3659-2018.

Vicca, S., Janssens, I.A., Flessa, H., Fiedler, S., Jungkunst, H.F., 2009. Temperature dependence of greenhouse gas emissions from three hydromorphic soils at different groundwater levels. Geobiology 7 (4), 465–476. https://doi.org/10.1111/j.1472-4669.2009.00205.x.

Volodin, E.M., 2007. Atmosphere-ocean general circulation model with the carbon cycle. Izvestiya - Atmospheric and Ocean Physics 43 (3), 266–280. https://doi.org/10.1134/S0001433807030024.

von Lützow, M., Kögel-Knabner, I., 2009. Temperature sensitivity of soil organic matter decomposition-what do we know? Biol. Fertil. Soils 46 (1), 1–15. https://doi.org/10.1007/s00374-009-0413-8.

Wang, B., Li, X., Ma, C.F., Zhu, G.F., Luan, W.F., Zhong, J.T., et al., 2022. Uncertainty analysis of ecosystem services and implications for environmental management – an experiment in the Heihe River basin. China. Science of the Total Environment 821, 153481. https://doi.org/10.1016/j.scitotenv.2022.153481.

Wang, H., Li, X., Xiao, J., Ma, M., Tan, J., Wang, X., Geng, L., 2019. Carbon fluxes across alpine, oasis, and desert ecosystems in northwestern China: the importance of water availability. Sci. Total Environ. 697, 133978 https://doi.org/10.1016/j.scitotenv.2019.133978.

Wang, J., Quan, Q., Weinan, C., Dashuan, T., Philippe, C., W, C.T., C, M.M, Benjamin, P., Hanqin, T., Yiqi, L., Xuefa, W., Guirui, Y., Shuli, N., 2021. Increased CO2 emissions surpass reductions of non-CO2 emissions more under higher experimental warming in an alpine meadow. Sci. Total Environ. 769, 144559.

Wang, T., Istanbulluoglu, E., Lenters, J., Scott, D., 2009. On the role of groundwater and soil texture in the regional water balance: an investigation of the Nebraska Sand Hills, USA. Water Resour. Res. 45, 1–13. https://doi.org/10.1029/2009WR007733.

Wang, W., Peng, S., Wang, T., Fang, J., 2010b. Winter soil CO2 efflux and its contribution to annual soil respiration in different ecosystems of a forest-steppe ecotone, North China. Soil Biol. Biochem. 42 (3), 451–458. https://doi.org/10.1016/j.soilbio.2009.11.028.

Wang, X., Piao, S., Ciais, P., Janssens, I.A., Reichstein, M., Peng, S., Wang, T., 2010a. Are ecological gradients in seasonal Q10 of soil respiration explained by climate or by vegetation seasonality? Soil Biol. Biochem. 42 (10), 1728–1734. https://doi.org/10.1016/j.soilbio.2010.06.008.

Wang, Y., Song, C., Yu, L., Mi, Z., Wang, S., Zeng, H., et al., 2018. Convergence in temperature sensitivity of soil respiration: evidence from the Tibetan alpine grasslands. Soil Biol. Biochem. 122 (January), 50–59. https://doi.org/10.1016/j.soilbio.2018.04.005.

Wen, X., Yu, G., Sun, X., Li, Q., Liu, Y., Zhang, L., et al., 2006. Soil moisture effect on the temperature dependence of ecosystem respiration in a subtropical Pinus plantation of southeastern China. Agric. For. Meteorol. 137, 166–175. https://doi.org/10.1016/j.agrformet.2006.02.005.

Wieder, W., Boehner, J., Bonan, G., 2014. Global biogeochemical cycles in earth system models with observations. AGU Publications 211–222. https://doi.org/10.1002/2013GB004665.Received.

Wu, D., Liu, S., Wu, X., Yang, X., Xu, T., Xu, Z., Shi, H., 2021a. Diagnosing the temperature sensitivity of ecosystem respiration in northern high-latitude regions. J. Geophys. Res. Biogeo. 1–19 https://doi.org/10.1029/2020jg005998.

Wu, D., Liu, S., Wu, X., Xu, T., Xu, Z., He, X., Shi, H., 2023. Evaluation of the intrinsic temperature sensitivity of ecosystem respiration in typical ecosystems of an endorheic river basin. Agric. For. Meteorol. 333 (July 2022), 109393 https://doi.org/10.1016/j.agrformet.2023.109393.

Wu, Q., Ye, R., Bridgham, S.D., Jin, Q., 2021b. Limitations of the Q10 coefficient for quantifying temperature sensitivity of anaerobic organic matter decomposition: A modeling based assessment. J. Geophys. Res. Biogeo. 126 (8), 1–18. https://doi.org/10.1029/2021JG006264.

Wutzler, T., Lucas-Moffat, A., Migliavacca, M., Knauer, J., Sickel, K., Šigut, L., et al., 2018. Basic and extensible post-processing of eddy covariance flux data with REddyProc. Biogeosciences 15 (16), 5015–5030. https://doi.org/10.5194/bg-15-5015-2018.

Xu, Z., Liu, S., Li, X., Shi, S., Wang, J., Zhu, Z., et al. (2013). Intercomparison of surface energy flux measurement systems used during the HiWATER-MUSOEXE. J. Geophys. Res. Atmos., 118(23), 13,140-13,157. https://doi.org/10.1002/2013JD020260.

Yan, T., Song, H., Wang, Z., Teramoto, M., Wang, J., Liang, N., et al., 2019. Temperature sensitivity of soil respiration across multiple time scales in a temperate plantation forest. Sci. Total Environ. 688 (5), 479–485. https://doi.org/10.1016/j.scitotenv.2019.06.318.

Yang, L., Zhang, Q., Ma, Z., Jin, H., Chang, X., Marchenko, S.S., Spektor, V.V., 2021. Seasonal variations in temperature sensitivity of soil respiration in a larch forest in the northern Daxing'an mountains in Northeast China. J. For. Res. 0123456789 https://doi.org/10.1007/s11676-021-01346-4.

Yang, R.M., Zhang, G.L., Liu, F., Lu, Y.Y., Yang, F., Yang, F., et al., 2016. Comparison of boosted regression tree and random forest models for mapping topsoil organic carbon concentration in an alpine ecosystem. Ecol. Indic. 60, 870–878. https://doi.org/10.1016/j.ecolind.2015.08.036.

Yu, H., Cui, Y., Li, S., Kang, S., Yao, Z., Wei, Z., 2023. Estimation of the deep drainage for irrigated cropland based on satellite observations and deep neural networks. Remote Sens. Environ. 298, 113819 https://doi.org/10.1016/j.rse.2023.113819.

Yvon-Durocher, G., Caffrey, J.M., Cescatti, A., Dossena, M., Giorgio, P. Del, Gasol, J.M., et al., 2012. Reconciling the temperature dependence of respiration across timescales and ecosystem types. https://doi.org/10.1038/nature11205.

Zhang, Y., Zhu, G., Yin, L., Ma, L., Xu, C., Chen, H., Ma, T., 2022. Optimal soil water content and temperature sensitivity differ among heterotrophic and autotrophic respiration from oasis agroecosystems. Geoderma 425 (August), 116071. https://doi.org/10.1016/j.geoderma.2022.116071.

Zhou, T., Shi, P., Hui, D., Luo, Y., 2009. Global pattern of temperature sensitivity of soil heterotrophic respiration (Q10) and its implications for carbon-climate feedback. J. Geophys. Res. Biogeo. 114 (2), 1–9. https://doi.org/10.1029/2008JG000850.